Soft spin waves and magnetization reversal in elliptical Permalloy nanodots: Experiments and dynamical matrix results

F. Montoncello,[1] L. Giovannini,[1] F. Nizzoli,[1] P. Vavassori,[1,2] M. Grimsditch,[3] T. Ono,[4] G. Gubbiotti,[5] S. Tacchi,[5] and G. Carlotti[5,2]
[1]*Dipartimento di Fisica, Università di Ferrara, Via Saragat 1, I-44100 Ferrara, Italy*
[2]*Research Center INFM-CNR S3, I-44100 Modena, Italy*
[3]*Materials Science Division, Argonne National Laboratory, Argonne, Illinois 60439, USA*
[4]*Institute for Chemical Research, Kyoto University, Uji 611-0011, Japan*
[5]*CNISM, Dipartimento di Fisica, Università di Perugia, Via A. Pascoli, I-06123 Perugia, Italy*
(Received 22 June 2007; published 19 July 2007)

We present an experimental and theoretical investigation of magnetization reversal in Permalloy elliptical nanodots under the application of a varying (quasistatic) magnetic field directed along the hard (short) and easy (long) axes of the ellipses. The magnetic response of the particles is investigated with the magneto-optic Kerr effect (MOKE) and Brillouin scattering (BLS). Experimental MOKE results are reproduced by micromagnetic simulations. The spectrum of the normal modes, calculated with the dynamical matrix method, reproduces the BLS results. We find that when an abrupt magnetization switching occurs it is accompanied by a soft magnetic mode (different in the two cases), the symmetry of which determines the initial steps (onset) of the microscopic reversal path.

DOI: 10.1103/PhysRevB.76.024426 PACS number(s): 75.75.+a, 75.60.Jk, 75.40.Mg, 78.35.+c

I. INTRODUCTION

The study of the magnetization reversal of small, submicron, ferromagnetic particles has been the focus of considerable recent activity.[1] The reasons for this flurry of activity are that (i) these particles have a size that is comparable to intrinsic magnetic lengths (e.g., exchange length, domain wall thickness) and hence one might expect their behavior to be different from that of bulk material, (ii) the technology-driven push to increase the density of magnetic storage media gives these systems potential technological importance, and last but not least, (iii) improvements in lithographic techniques for sample fabrication made it possible to routinely fabricate these small structures with considerable precision and reproducibility.

Understanding and controlling the magnetic equilibrium state is important both from a fundamental standpoint and for technological applications. Since the magnetic configuration at remanence, which is likely to be crucial in any application, is a function of both particle geometry and field history, it is therefore also important to understand how these factors determine the magnetic response of the particle. Micromagnetic simulations are currently performed to investigate such effects, over a broad range of parameter space: particle size and geometry, material parameters, and field histories.[2] A wide variety of behaviors are observed that include reversal via vortex nucleation and annihilation, domain wall nucleation and motion, and coherent rotation. Micromagnetic simulations have also cataloged some of the precursor states prior to reversal: flower state, onion state, *C* state, *S* state, etc.[3–5] One of the issues that makes magnetization reversal such a complex phenomenon is that, even for the same precursor state (e.g., a *C* state), different particles reverse via different routes, e.g., a stripe domain for a rectangular particle[6] and a vortex state for a disk.[7] However, micromagnetic simulations do not provide a microscopic explanation why one reversal mechanism is preferred to another when the system undergoes a transition between equilibrium states under the action of the applied field.

In this paper we show that explicit calculations of the spin normal modes of submicrometric magnetic particles can answer the question above: when a particle changes state in a discontinuous way the magnetic configurations during reversal are intimately related to, and determined by, the symmetry of a soft spin excitation. In particular, we show that there is a correlation between the soft mode, its symmetry, and the initial stages of magnetization reversal. We demonstrate this statement for an elliptical particle under an external field applied along either the hard or easy axis by studying both theoretically and experimentally the field dependence of the normal modes together with the longitudinal and transverse hysteresis loops.

The paper is organized as follows. The samples and the experimental techniques are described in Sec. II. In Sec. III we present the experimental and calculated results, for both the static and dynamic magnetic properties, as a function of the magnitude and direction of the magnetic field, applied along the hard axis of the ellipses. In particular we describe in detail the correlation between the magnetization reversal process and the soft spin mode. A similar analysis is carried out in Sec. IV for the easy axis. Conclusions are drawn in Sec. V.

II. SAMPLES AND EXPERIMENTAL TECHNIQUES

The sample consists of a rectangular array of 15-nm-thick Permalloy ($Ni_{80}Fe_{20}$) cylindrical dots with elliptical cross section, fabricated by electron-beam lithography followed by a lift-off process on thermally oxidized Si. Our elliptical dots have 500- and 200-nm axes and an interdot separation of 200 nm (edge to edge) in both in-plane directions.[8] Therefore, to a good approximation, the ellipses can be considered as noninteracting. Scanning electron microscopy and atomic force microscopy confirmed that the morphology of the pat-

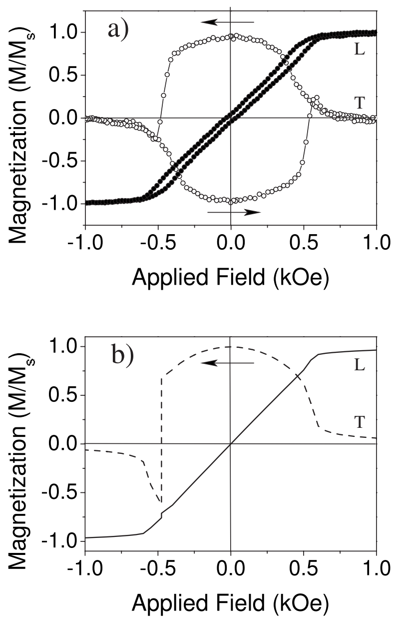

FIG. 1. Longitudinal (L) and transverse (T) hysteresis loops for elliptical particles. The field is applied along the hard (short) axis. Upper panel (a) contains the V-MOKE experimental results. Solid symbols: L component. Open symbols: T component. Lower panel (b) shows the results of simulations with the applied field varying from positive to negative values. Solid line: L component. Dashed line: T component. The applied field is slightly misaligned (1°) from the hard axis. Noteworthy is the sharp jump in the transverse component at about $H=-0.5$ kOe.

terns was of good quality, concerning both dimensional control and uniformity. The spectrum of magnetic normal modes has been measured using Brillouin scattering (BLS) performed in air at room temperature at the GHOST Laboratory, University of Perugia[9] in backscattering geometry using a Sandercock-type 3+3 pass tandem interferometer. The BLS spectra were recorded consecutively while stepwise decreasing a dc magnetic field $\boldsymbol{H}$ applied along one of the axis of the ellipse and perpendicular to the scattering plane of light. The 532-nm light of a solid-state laser, providing a single-mode power of 200 mW on the sample surface, was used in the experiment at an incidence angle of 10°. The magnetostatic behavior of the sample has been characterized using a vectorial magneto-optic Kerr effect magnetometry (V-MOKE).[10] V-MOKE measurements probe both in-plane components of magnetization, parallel to the external field $\boldsymbol{H}$ (longitudinal magnetization) and orthogonal to it (transverse magnetization).

III. MAGNETIC FIELD ALONG THE HARD AXIS

The measured and calculated hysteresis loops for the field along the hard (short) axis are shown in Fig. 1. In this case a full understanding of the magnetization reversal requires the investigation not only of the behavior of the longitudinal component of the magnetization but also of the transverse one. Indeed, the transverse loop indicates that, as the field is reduced from a large positive value, the magnetization $\boldsymbol{M}$ rotates away from the hard axis and becomes fully aligned along the easy axis at $H=0$. We note that neither the measured nor calculated loops show any evidence of a discontinuity at positive fields where "reversal" is initiated. However, after the field has become negative, the transverse magnetization shows a sharp jump and a change of sign at about -0.5 kOe. The calculated hysteresis half-loop shown in Fig. 1(b) has been obtained by using the OOMMF micromagnetic simulator.[11] The equilibrium states for any applied field were used as starting points for the normal-mode calculations presented below. In the present simulations the particle is built out of small cells, of size $5\times5\times15$ nm^3. The material parameters are saturation magnetization $M_s=800$ G, exchange stiffness $A=1.3$ μerg/cm, and gyromagnetic ratio $\gamma=2.95$ GHz/kOe. From simulations we find that when the field is aligned *exactly* along the hard axis the reversal process is microscopically very different from that when the field is misaligned even by a fraction of 1°. We attribute these dramatic changes to the symmetry-breaking effect of the misaligned field. However, since experimentally exact alignment is not achievable, all simulations described here were performed with the field applied at 1° from the hard axis.

The BLS experimental results for the field applied along the hard axis are shown by the symbols in Fig. 2. The measurements have been done with the applied field varying from positive to negative values. The solid symbols denote the most intense peak in the BLS spectra; other peaks are shown with open symbols. To compare with these data, we have calculated the spin waves of a single elliptical magnetic particle by using the dynamical matrix method that we have recently developed[12] and successfully used to describe the spin excitations of nanoparticles, such as circular dots[13] and rings.[14] In this framework the mode frequencies and the magnetization profiles are calculated from the dynamical matrix. This method, working directly in the frequency domain, differs from those in the time domain, based on the Fourier transform of the time behavior of the magnetization.[15] Our method is particularly suitable to compare with the BLS results, insofar as it gives in a single calculation the thermally excited spin modes of any symmetry and allows the BLS cross section to be calculated.[8] To describe the results of our normal-mode calculations we will use the classification scheme proposed in Ref. 8, where elliptical dots were investigated by varying the in-plane direction of the applied field for a fixed magnitude, high enough to induce sample saturation. There the modes were classified as follows. Excitations with n nodes along and perpendicular to the applied field are called backwardlike modes (n-BA) and Damon-Eshbach-like modes (n-DE), respectively, the $n=0$ mode of both these series is called the Fundamental (F), and modes with amplitude localized at the ends or edges are called end modes (EM). There are also mixed modes that are combinations of the above.

The solid lines in the figure are the calculated modes that have non-negligible Brillouin cross section, according to the expression given in Ref. 8. The bold solid line is the mode with the largest calculated intensity. Since the F mode, the one observable in ferromagnetic resonance (FMR), is expected to have the largest cross section for these BLS experiments, we also plot with a dash-dotted line the frequency of

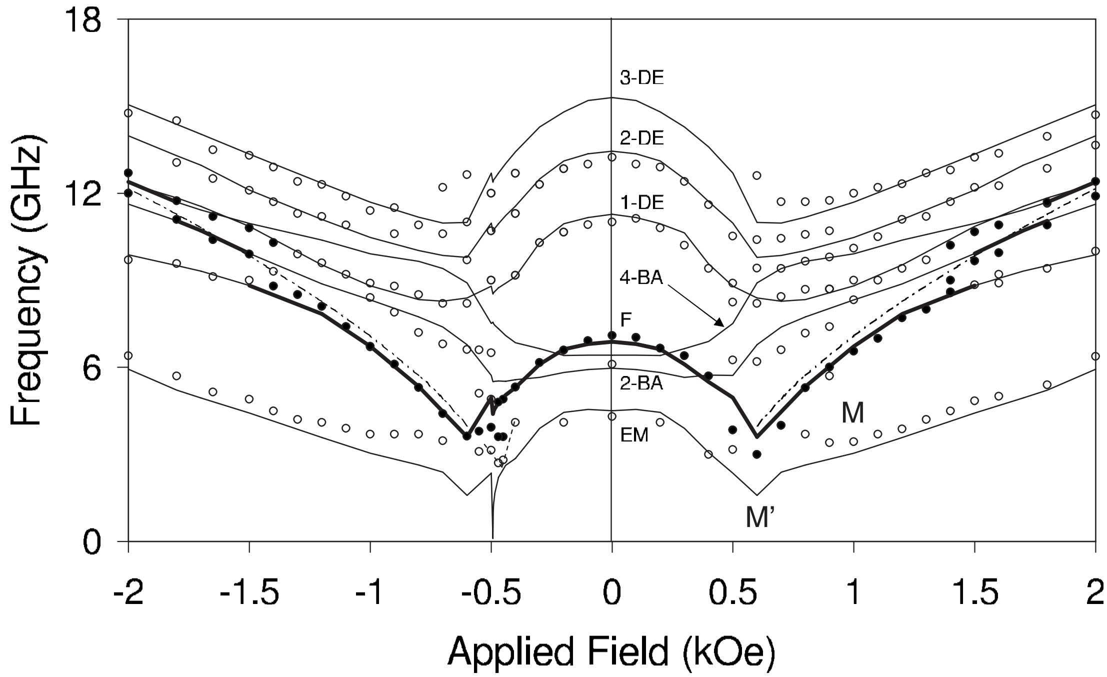

FIG. 2. Spin-wave mode frequencies vs applied field along the hard axis. The symbols represent experimental Brillouin data; solid circles the modes with the highest intensity peaks in the spectra, open circles other modes. The solid lines are the results obtained from the calculations; the modes which exhibit the character of the fundamental one are shown by thick lines. The dash-dotted line shows the calculated frequency of the ferromagnetic resonance of the equivalent ellipsoid. Notable is the soft EM at about −0.5 kOe found in the simulations and also observed in the measurements (marked by a dashed line connecting a few experimental points, as a guide for the eye).

the fundamental mode of an equivalent three-dimensional (3D) ellipsoid.[16] The excellent agreement between the bold line and the solid symbols attests to the accuracy of our simulations. Additionally, comparison with the FMR equation indicates that the F mode hybridizes with the 2-BA and 4-BA modes as the field is varied in the range 1.3–2 kOe.[8] In this field region none of the calculated mode profiles resembles a pure F mode, thus explaining the discontinuous behavior of the intense peak. The discrepancy between the positions of the frequency minimum of the EM in Fig. 2 (label M for the experimental data and label M' for simulation) is not surprising because the calculated frequency of the EM is known to depend critically on the exact shape of the dot edges.[13]

We now turn our attention to the sharp softening at about −0.5 kOe, where the calculated EM approaches zero frequency. Notably this softening occurs at the same field where the jump in the transverse magnetization is observed in Fig. 1. Experimentally the frequency minimum appears as a small dip at $H=-0.47$ kOe; this is emphasized by the V-shaped cusp shown in Fig. 2 and in the closer view of Fig. 3(b) (dashed line). Figure 3(a) shows a BLS spectrum taken at that field, where the EM is clearly visible at about 2.8 GHz, especially on the Stokes side (peak C). We suggest that the reason why the measured minimum does not drop below this frequency, as predicted by the calculation, is due to the narrow range where the softening occurs [see Fig. 3(b)] and to the statistical distribution of the physical properties of the particles in the array (the illuminated area involves a few thousands ellipses). For the same reason, in the neighbor-

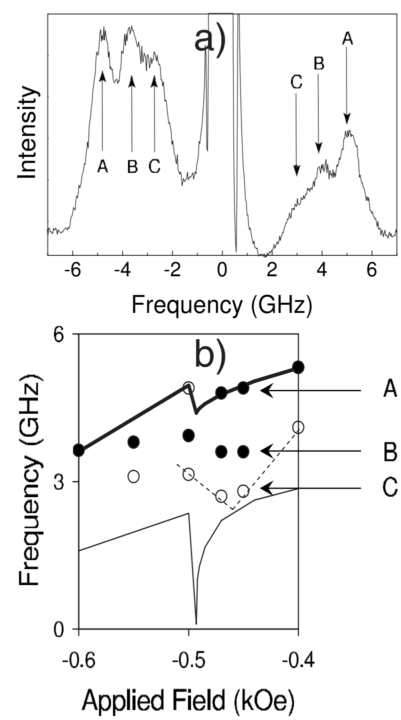

FIG. 3. (a) A low-frequency portion of the BLS spectrum measured at $H=-0.47$ kOe. (b) Enlargement of Fig. 2 showing the low-frequency modes in the range $H=(-0.6,-0.4)$ kOe. The arrows and the letters A, B, and C point to three modes discussed in the text. The dashed line is a guide for the eye, connecting a few experimental points.

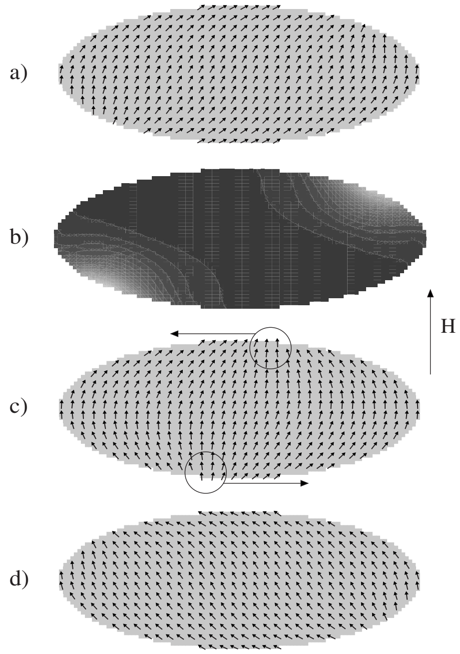

FIG. 4. Field $\boldsymbol{H}$ applied along the hard axis. (a) Equilibrium S-like state calculated at $H=-0.493$ kOe. (b) Profile of the soft mode (magnetization component parallel to the long axis of the ellipse) calculated in the equilibrium state (a); white and black denote large and zero amplitude, respectively. (c) A snapshot of the spin configuration (asymmetric onion) during the transformation. The two circles highlight the "localized domain walls" that propagate as indicated by the arrows in the upper and lower parts of the sample. (d) Final ground state at $H=-0.5$ kOe.

hood of the transition, ellipses with reversed and nonreversed magnetization states may coexist. This conjecture is experimentally confirmed by the simultaneous presence of two intense peaks at 3.6 and 4.9 GHz in the BLS spectra taken at -0.47 kOe [labeled A and B in Figs. 3(a)] that correspond to the F modes of the two phases.

Having firmly established that the simulations correctly account for the experimental results, we can interpret with confidence not only the mode frequencies but also their profiles. Note that the latter are not accessible in the experiments. Specifically we will show how the symmetry of the soft mode determines the reversal path. Figure 4(a) shows the S state at $H=-0.493$ kOe just prior to the transition, and Fig. 4(b) is the mode profile of the soft EM in this equilibrium state. The white regions indicate large spin amplitudes; the spins in the black regions have small or zero amplitude. Upon reducing H just beyond the critical field marking the transition, the spin-restoring torque vanishes and the end mode goes soft (viz., reaches zero frequency). When this occurs the spins in the white regions react to this instability by rotating counterclockwise. The subsequent evolution of the spin configuration is shown in Fig. 4(c); note that this state is not stable and is simply a snapshot at a given instant. The evolution of the original equilibrium state [Fig. 4(a)] can best be described as the motion of two "localized domain walls" [indicated by the two circles in Fig. 4(c)] that migrate as indicated by the arrows until they again reach equilibrium in the state shown in Fig. 4(d) that is the ground state calculated at $H=-0.5$ kOe. This instability is therefore associated with a transition from an S-like state (top and bottom spins pointing to the right), through an unstable asymmetric "onionlike" state [Fig. 4(c)], to a reversed-S-like state (top and bottom spins pointing to the left). The change from right-to left-pointing spins is responsible for the discontinuity in the transverse magnetization. Note that the state (a) and, in particular, state (c) have the same (inversion) symmetry as the soft mode. Specifically, the magnetization behaves as an axial vector. Considering that the transient state (c) at the onset of the transition originates from a dynamic instability as described above, it is reasonable to expect its symmetry to be the same as that of the soft mode. It is worth noting here that the symmetry of the mode going soft can be different from that of the initial state prior to the transition.[6] However, also in the latter case, the symmetry relationship between soft mode and transient state outlined above is verified, so that we can conclude that it is a general rule.

It is interesting to compare the soft-mode behavior described above with the frequency minimum (not zero) in the calculated EM dispersion at $H=0.6$ kOe, which corresponds to the beginning of reversal, defined as the onset of substantial changes in $\boldsymbol{M}$. The calculations indicate that this frequency minimum does not correspond to a true soft-mode softening (i.e., there is no mode frequency going to zero). Indeed the results in Figs. 1 and 2 indicate that reversal begins without any discontinuity in the magnetization and thus is not driven by any dynamic instability, at variance with the previous case. We attribute this to the absence of any change of symmetry during the initial stages of reversal at positive fields. Due to the field misalignment, even at the highest fields the ground-state symmetry is that of an S state. As the field is lowered the S shape simply deforms continuously—keeping its S-like character—so that the initial stage of reversal is achieved by a "coherent rotation" of an S state. Conversely, we have found that, without misalignment, the calculated EM exhibits in the positive field region a soft-mode behavior when the mirror symmetry of the "perfect onion state" breaks down, leading to a distorted lower-symmetry state. However, such an experiment is not feasible since it is practically impossible to perfectly align the external field along the ellipse's short axis.

IV. MAGNETIC FIELD ALONG THE EASY AXIS

The measured and calculated longitudinal hysteresis loops when the field is applied along the easy (long) axis of the ellipse are shown in Fig. 5. In this case neither the calculations nor the experiment show an appreciable transverse component of the magnetization. The easy-axis experimental data indicate that reversal is discontinuous, with nucleation fields in the range 0.36–0.48 kOe. For particles of this shape and size it is known that the reversal process includes the nucleation and annihilation of vortices.[17] Our micromagnetic simulation of Fig. 5(b) (with a 1° misalignment of the applied field with respect to the symmetry axis) gives a nucleation field of 0.44 kOe. Simulations without misalignment would give a nonrealistic higher nucleation field. Therefore the 1° misalignment has been also adopted for the dynamic

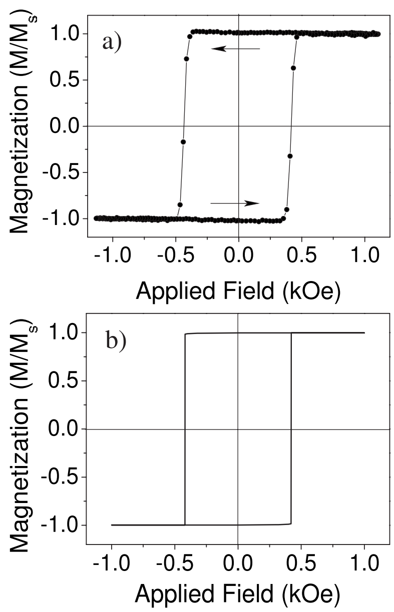

FIG. 5. Longitudinal hysteresis loops for elliptical particles. The field is applied along the easy (long) axis. (a) V-MOKE experimental results. (b) Results of simulations. The applied field is slightly misaligned (1°) from the easy axis.

calculations, performed with the same method used as in the previous section.

The BLS experimental results for the field applied along the easy axis are shown by the symbols in Fig. 6. The measurements have been done with the applied field varying from positive to negative values. Overall there is good agreement between the measured and calculated frequencies. Only the dispersions of the calculated modes that exhibit an appreciable cross section have been shown. The measured spectra are also consistent with the Kerr loop, showing a discontinuous behavior of the mode frequencies at about −0.36 kOe, corresponding to the onset of the magnetization reversal. Similarly to what found for the hard axis (see the discussion of the transition at H=−0.493 kOe in the previous section)

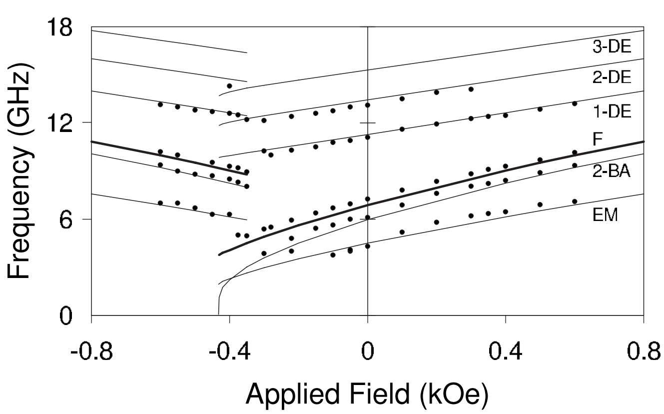

FIG. 6. Spin-wave mode frequencies vs applied field along the easy axis. The symbols represent experimental Brillouin data. The solid lines are the results obtained from the calculations; the mode which exhibits the character of the fundamental one (F) is shown by thick lines.

there is evidence from the spectra that in a small field range around this value spin modes of the two opposite states coexist. This is not surprising due to the expected spread of the physical properties and alignment of the dots in the array. For this reason the calculated dispersions of Fig. 6 for the reversed phase have been extended from −0.43 kOe to −0.36 kOe, to compare with the experimental data. As required by symmetry the frequencies below −0.36 kOe are equal to those above 0.36 kOe. The comparison between the measured and calculated dispersions of Fig. 6 allows us to identify five modes: from the bottom, the EM, the symmetric 2-BA mode, the fundamental mode, and two DE modes. It can be seen in the figure that, at a field just below −0.4 kOe, the 2-BA mode becomes the lowest-frequency mode of the particle, even lower than the EM. We stress that none of the thousands of the other modes, which are not shown in Fig. 6 for clarity, have lower frequency either. The 2-BA mode reaches zero frequency at about −0.44 kOe, indicating the onset of the instability, and is referred to as the soft mode. Although the measured intensity of the EM and 2-BA peaks becomes negligible below 3 GHz, so that no BLS experimental information is available in this low-frequency range, the fast decreasing trend of the data points relative to the 2-BA mode plotted in Fig. 6 is consistent with the theoretically predicted softening of this mode below −0.4 kOe. When H reaches the nucleation field, all the modes undergo a remarkable jump due to the change of state; in particular, the mode frequencies are much higher in the reversed (ground) state than in the metastable state prior to reversal.

In order to show that the 2-BA soft mode triggers the magnetization reversal and determines the (initial) path of the reversal process, we compare in Fig. 7 the profile of this mode with the various states across the transition. In Fig. 7(a) we show the equilibrium state of the magnetization just before reversal (H=−0.43 kOe). Note that, visibly, the magnetization field presents a S-like structure imposed by the misaligned applied field. In Fig. 7(b) we show the amplitude profile of the 2-BA mode calculated at the same field (viz., dynamic magnetization component δm_x perpendicular to the easy axis). We note that the spins in the black and white areas are out of phase. Figures 7(c) and 7(d) are two snapshots of the magnetization field obtained during the reversal process when the applied field is H=−0.44 kOe (nucleation field). We stress that these two last configurations are unstable and represent only transient states of the particle magnetization. In Fig. 7(c) one can observe that the clockwise twist region, with respect to the initial configuration of panel (a), approximately corresponds to the white area in Fig. 7(b) while the spins in the black areas have rotated counterclockwise near the particle tips. As in the previous case (hard axis), the transient state of Fig. 7(c) at the beginning of the transition presents the same symmetry of the soft mode, both of them being invariant with respect to space inversion. Subsequent evolution of the system is clearly outside of the range of validity of the normal-mode picture which is valid only for small amplitudes. However, once the process is initiated, the twists evolve into two vortices that nucleate on the opposite sides of the particle [Fig. 7(d)]. The vortices travel across the sample, as indicated by the arrows in Fig. 7(d), annihilate on the opposing side, and result in a reversed mag-

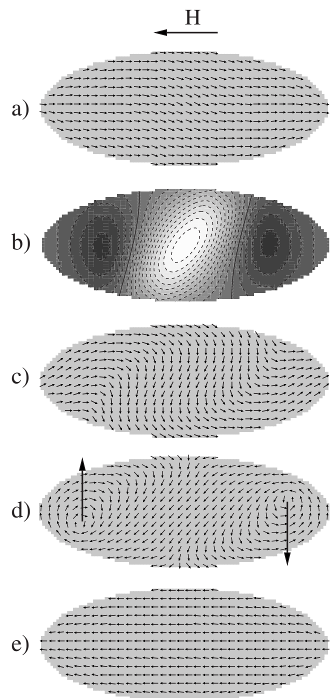

FIG. 7. Field ***H*** applied along the easy axis. (a) Equilibrium *S*-like state calculated at −0.43 kOe. (b) Profile of the soft mode (magnetization component δm_x normal to the long axis of the ellipse) calculated in the equilibrium state above; white and black denote large positive and negative values, respectively; the nodes are marked by a solid contour line. (c),(d) Two snapshots of the magnetization configuration during the reversal process when the applied filed is $H = -0.44$ kOe. The arrows in panel (d) show the direction of motion of the vortices. (e) Final ground state at $H = -0.44$ kOe.

netization state, as in panel (e). It is also interesting to note that the 2-BA-mode precession close to the reversal is strongly elliptic, i.e., $|\delta m_x| \gg |\delta m_y|$, to a much larger extent than far from the transition. We then conclude that the dynamics of the reversal process provided by micromagnetism in the time domain, through integration of the Landau-Lifshitz-Gilbert equation, is explained by an instability of the excitation spectrum calculated in the metastable equilibrium state prior to the onset of the reversal process.

V. CONCLUSIONS

In conclusion, magnetization reversal in small elliptical particles with a field applied at a small angle to the hard (short) axis is a continuous and reversible process during the initial stages, reversal being achieved by coherent rotation of an *S*-like state. Only at a negative field does a soft spin mode trigger a transition from an *S*-like to a reversed-*S*-like state; this first-order transition has little effect on the longitudinal hysteresis loop but produces a large discontinuity in the transverse loop. We have shown that, microscopically, the controlling factor determining the initial steps of the reversal process is the symmetry of the soft spin mode, which in this case turned out to be an end mode. For the same ellipse with the field applied at a small angle to the easy (long) axis, a backwardlike mode becomes soft and its symmetry is responsible for the microscopic path that forces the system to nucleate vortices and eventually to reverse. We conclude that whenever in a reversal process there is a change in the symmetry of one of the equilibrium states through which the system evolves, that change is determined by a mode that becomes soft. We believe this provides insight into the general problem of magnetization reversal. This is not only interesting from a fundamental standpoint, but may also lead to techniques for writing specific magnetic states into patterned media.

ACKNOWLEDGMENTS

We thank T. Okuno for sample preparation and R. Zivieri and M. G. Pini for useful discussions. F.M., L.G., F.N., and P.V. acknowledge support from the Project NANO&NANO of the University of Ferrara.

[1] *Spin Dynamics in Confined Magnetic Structures III*, edited by B. Hillebrands and A. Thiaville (Springer, Berlin, 2006).
[2] S. L. Whittenburg, in *Magnetic Nanostructures*, edited by H. S. Nalwa (American Scientific, Stevenson Ranch, CA, 2002), p. 425.
[3] M. E. Schabes, J. Magn. Magn. Mater. **95**, 249 (1991).
[4] H. Kronmüller and R. Hertel, J. Magn. Magn. Mater. **215-216**, 11 (2000).
[5] N. A. Usov, Ching-Ray Chang, and Zung-Hang Wei, Phys. Rev. B **66**, 184431 (2002).
[6] G. Leaf, H. Kaper, M. Yan, V. Novosad, P. Vavassori, R. E. Camley, and M. Grimsditch, Phys. Rev. Lett. **96**, 017201 (2006).
[7] R. P. Cowburn, D. K. Koltsov, A. O. Adeyeye, M. E. Welland, and D. M. Tricker, Phys. Rev. Lett. **83**, 1042 (1999).
[8] G. Gubbiotti, G. Carlotti, T. Okuno, M. Grimsditch, L. Giovannini, F. Montoncello, and F. Nizzoli, Phys. Rev. B **72**, 184419 (2005).
[9] http://ghost.fisica.unipg.it
[10] P. Vavassori, Appl. Phys. Lett. **77**, 1605 (2000); F. Carace, P. Vavassori, G. Gubbiotti, S. Tacchi, M. Madami, G. Carlotti, and T. Okuno, Thin Solid Films **515**, 727 (2006).
[11] M. J. Donahue and D. G. Porter, *OOMMF Users Guide, Version 1.0* (NIST, Gaithersburg, MD, 1999).
[12] M. Grimsditch, L. Giovannini, F. Montoncello, F. Nizzoli, G. K. Leaf, and H. G. Kaper, Phys. Rev. B **70**, 054409 (2004).
[13] L. Giovannini, F. Montoncello, F. Nizzoli, G. Gubbiotti, G. Carlotti, T. Okuno, T. Shinjo, and M. Grimsditch, Phys. Rev. B **70**, 172404 (2004).
[14] G. Gubbiotti, M. Madami, S. Tacchi, G. Carlotti, H. Tanigawa, T. Ono, L. Giovannini, F. Montoncello, and F. Nizzoli, Phys. Rev. Lett. **97**, 247203 (2006).
[15] R. D. McMichael and M. D. Stiles, J. Appl. Phys. **97**, 10J901 (2005).
[16] A. Morrish, *The Physical Principles of Magnetism* (Wiley, New York, 1965).
[17] P. Vavassori, N. Zaluzec, V. Metlushko, V. Novosad, B. Ilic, and M. Grimsditch, Phys. Rev. B **69**, 214404 (2004).